



ELSEVIER

Contents lists available at ScienceDirect

## Journal of Magnetism and Magnetic Materials

journal homepage: [www.elsevier.com/locate/jmmm](http://www.elsevier.com/locate/jmmm)

# Observation of the dynamics of magnetic nanoparticles induced by a focused laser beam by using dark-field microscopy

Hai-Dong Deng<sup>a,\*</sup>, Guang-Can Li<sup>b</sup>, Hai Li<sup>a</sup><sup>a</sup> Department of Applied Physics, College of Science, South China Agricultural University, Guangzhou 510642, China<sup>b</sup> Laboratory of Nanophotonic Functional Materials and Devices, School of Information and Optoelectronic Science and Engineering, South China Normal University, Guangzhou 510006, China

## ARTICLE INFO

## Article history:

Received 26 November 2013

Received in revised form

19 February 2014

Available online 5 April 2014

## Keywords:

Magnetic nanoparticles

Dissipative force

Soret coefficient

## ABSTRACT

The dynamics of Fe<sub>3</sub>O<sub>4</sub> magnetic nanoparticles under the irradiation of a tightly focused laser beam was investigated by using a high-intensity dark-field microscopy. A depletion region of magnetic nanoparticles was found at the center of the laser beam where the dissipative force (absorption and scattering forces) dominated the dynamics of the magnetic nanoparticles. In contrast, the dynamics of magnetic nanoparticles was dominated by thermal and mass diffusions at the edge of the laser beam where the dissipative force was negligible. In addition, the transient variation in the concentration of magnetic nanoparticles was characterized by recording the transient scattering light intensity. The coefficients of thermal diffusion, mass diffusion and the Soret effect for this kind of magnetic nanoparticles were successfully extracted by using this technique.

© 2014 Elsevier B.V. All rights reserved.

## 1. Introduction

In the past decades, Magneto-optical effects of magnetic fluids have attracted great interest due to the potential applications in the construction of diverse functional devices such as magnetic field sensors [1–3], tunable gratings [4–6], optical filters [7,8], modulators [9–11], and switches [12,13]. Recently, a new technique that can be used to realize multi-sized nanospheres assembly or to form ordered three-dimensional optical crystals in magnetic fluids under magnetic fields has been reported [14–17]. Based on this technique, we have proposed a completely different method to assemble silica microspheres suspended in magnetic colloid into a three-dimensional crystal by utilizing the giant nonequilibrium depletion force induced by a single tightly focused laser beam [18]. The physical mechanism responsible for these phenomena is ascribed to the interaction of magnetic nanoparticles (MNPs) suspended in magnetic fluids with the tightly focused laser beam.

Early in 1998, Tabiryan et al. theoretically studied the interactions of MNPs with a laser light and experimentally investigated the Soret feedback effect in the thermal diffusion of MNPs by monitoring the transmission of the laser light [19]. Meanwhile, Lenglet et al. showed that the forced Rayleigh scattering could be used as an experimental tool to study the thermal dynamics of

MNPs suspended in colloids and to measure the Soret coefficient of MNPs covered with different surfactants [20]. Since the particle size of MNPs is generally in the range of several and several tens of nanometers, the direct observation of the dynamics of MNPs under the irradiation of tightly focused laser beam remains to be a challenge. In addition, the effect on the dynamics of MNPs induced by optical forces (e.g. scattering and absorbing forces) were not taken into account for simplicity in previous reports [19,20].

In this article, the dynamics of Fe<sub>3</sub>O<sub>4</sub> MNPs under the irradiation of focused laser beam was investigated by using dark-field microscopy. It is shown that a simple description of the interaction of focused laser beams and complex media based on thermal diffusion and mass diffusion is not adequate in many cases. It is revealed that the dynamics of MNPs is dominated by different mechanisms when MNPs are located at different areas of the focus laser beam. In addition, it is demonstrated that the Soret coefficient of MNPs can be extracted by recording the transient scattering light intensity.

## 2. Theory

The dynamics of MNPs after considering both mass and thermal diffusions can be written as follows [19]:

$$\frac{\partial c}{\partial t} = D \frac{\partial^2 c}{\partial r^2} - \frac{\sigma}{\chi \rho C_p} D_T c(1-c)l(r), \quad (1)$$

\* Corresponding author. Tel.: +86 159 2035 9682.

E-mail address: [dhdong@scau.edu.cn](mailto:dhdong@scau.edu.cn) (H.-D. Deng).

where  $c$  denotes the concentration of MNPs;  $D$  and  $D_T$  are the coefficients of mass diffusion and thermal diffusion, respectively;  $\chi$  is the thermal conductivity coefficient;  $I(r)$  is the intensity of the laser beam as a function of the displacement  $r$  from the laser spot center,  $\rho C_p$  is the heat capacitance of the MNPs, and  $\sigma$  is the absorption constant on the concentration of the MNPs. For small  $c$ , it can be simplified as

$$\sigma = \alpha c, \quad (2)$$

where  $\alpha$  is a constant. In this case, Eq. (1) can be rewritten as

$$\frac{\partial c}{\partial t} = D \frac{\partial^2 c}{\partial r^2} - \frac{\alpha}{\chi \rho C_p} D_T c^2 (1 - c) I(r). \quad (3)$$

Generally speaking, the mass diffusion of MNPs is induced by the thermal diffusion of MNPs, which in turn weakens the thermal diffusion. Thus, Eq. (3) can be further simplified by the process dominating the dynamics of MNPs. When the laser light is turned on, the thermal diffusion dominates the dynamics of MNPs while the mass diffusion can be neglected. Eq. (3) can be simplified as

$$\frac{\partial c}{\partial t} = -D_T c^2 (1 - c) \frac{\alpha I}{\chi \rho C_p} = \mu D_T c^2 (1 - c) I(r), \quad (4)$$

where,  $\mu = -(\alpha/\chi\rho C_p)$ . Integration of Eq. (4) yields

$$-\frac{1}{c} + \ln \frac{c}{1-c} = \mu D_T I(r) t + C_{cst} \ \& \ \frac{c}{1-c} \exp(-1/c) = A_0 \exp[\mu D_T I(r) t], \quad (5)$$

where  $C_{cst}$  is the integration constant and we set  $A_0 = \exp(C_{cst})$ . By substituting  $c(t=0, r) = c_0$  in Eq. (5), we can get

$$C_{cst} = -\frac{1}{c_0} + \ln \frac{c_0}{1-c_0}, \quad (6)$$

as shown in Eq. (5), the concentration of MNPs decreases exponentially with time after the laser light is turned on. If the exponential decay time  $t_1$ , which is defined as the time at which the concentration of MNPs is reduced to  $1/e$  of its initial value, can be extracted from the experimental results, then one can derive the thermal diffusion constant  $D_T$  of MNPs by

$$t_1 = -\frac{1}{\mu D_T I(r)} \Rightarrow D_T = -\frac{1}{\mu I(r) t_1}. \quad (7)$$

In the experiment, the scattering light intensity of MNPs can be used to characterize the concentration of MNPs. By recording the transient variation of scattering light intensity of MNPs,  $t_1$  can be easily extracted by fitting the scattering light intensity with exponential decay.

As reported by Lenglet et al. [19], the temperature gradient formed by the absorption of laser energy will vanish when MNPs move to the boundary of the laser spot due to thermal diffusion effect. In this case, the dynamics of MNPs is dominated by mass diffusion and some MNPs will move back to the laser spot center. Thus, Eq. (3) is simplified as

$$\partial c / \partial t = D \Delta c. \quad (8)$$

Here, our model considers only the two-dimensional (2D) case, the temperature gradient and the attenuation of the laser light intensity along the propagation direction are neglected. This assumption is reasonable and it allows us to capture the key feature of the dynamics of MNPs. Thus, we have

$$\frac{\partial c}{\partial t} = D \frac{\partial^2 c}{\partial r^2}. \quad (9)$$

here,  $c(0, r) = c_0(r)$ ,  $c(t, 0) = p_0$  and  $\lim_{r \rightarrow R} c(r, t) = c_0$ . The solution of Eq. (9) is

$$c(r, t) = A \lambda_n \exp(\lambda_n D t) \sum_1^{\infty} B_n \sin(\sqrt{-\lambda_n} r)$$

$$= \sum_1^{\infty} \left\{ C_n \exp[-\pi^2 n^2 D t / R^2] \sin \left[ \frac{\pi n r}{R} \right] \right\}, \quad (10)$$

here

$$c(r, 0) = \sum_1^{\infty} C_n \sin[(\pi n r) / R],$$

and

$$C_n = \frac{2}{R} \int_0^R c_0(r) \sin \left[ \frac{\pi n r}{R} \right] dr.$$

here,  $R$  denotes the size of the sample cell. For the right-side of Eq. (10), it is sufficient to consider the first term of the summation and one obtains

$$c(r, t) = C_1 \exp\left(-\frac{\pi^2 D t}{R^2}\right) \sin\left(\frac{\pi r}{R}\right). \quad (11)$$

The concentration of MNPs varies exponentially with time. By recording the scattering light intensity of MNPs, the time constant  $t_2$  for the mass diffusion of MNPs can be easily extracted by fitting the time-dependent scattering light intensity. Thus, we can derive the thermal diffusion constant  $D$  of MNPs by

$$t_2 = -\frac{R^2}{\pi^2 D} \Rightarrow D = -\frac{R^2}{\pi^2 t_2}. \quad (12)$$

### 3. Sample preparation and experimental details

The magnetic colloid used in our study was water-based  $\text{Fe}_3\text{O}_4$  fabricated by the chemical coprecipitation technique (Central Iron and Steel Research Institute, China). The average diameter of MNPs was measured to be  $\sim 12$  nm and the weight fraction of MNPs was determined to be 25.7%. In our experiments, the magnetic fluid was first diluted with water and the volume concentration of MNPs was  $1.75 \times 10^{16} \text{ cm}^{-3}$ . Then the magnetic colloid was sonicated for half an hour and sealed into a sample cell with a thickness of  $50 \mu\text{m}$ .

The 532-nm laser light from a solid-state laser (Verdi-5, Coherent) was focused on the sample cell by using a  $63 \times$  objective lens (NA=1.43) and the power of laser light was chosen to be 8 mW, as schematically shown in Fig. 1. The dynamics of MNPs was monitored by using an inverted dark-field microscopy (Axio Observer A1, Zeiss) in combination with a charge-coupled device (CCD). The concentration of MNPs was characterized by the scattering light intensity and 500 images of the scattering light were captured with the continuous capture mode of the CCD after the laser light had been turned on. The exposure time for each image was set to be 200 ms.

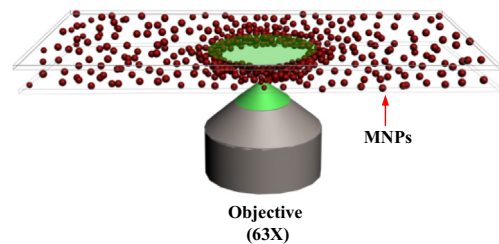


Fig. 1. Schematic showing the experimental setup used to investigate the dynamics of MNPs under the irradiation of focused laser light. (For interpretation of the references to color in this figure legend, the reader is referred to the web version of this article.)

#### 4. Results and discussions

Before the laser light was turned on, the MNPs were observed to distribute uniformly in the colloid, as shown in Fig. 2(a). Once the laser beam was turned on, the MNPs were rapidly pushed out of the laser spot and a depletion region was formed, which can be seen in Fig. 2(b) and (c). As predicted in Ref. [19], MNPs were observed to accumulate at the edge of the laser spot. However, no obvious Soret feedback effect was observed, especially at the center area of the laser spot. After the laser was turned off, MNPs began to drift to the depletion region and the distribution of MNPs became uniform again gradually, as shown in Fig. 2(e) and (f).

In order to gain a deep insight into the dynamics of MNPs under the irradiation of a focused laser beam, the scattering light images of MNPs were recorded at different times by using the dark-field microscopy. For quantitatively analyzing the concentration of MNPs which was represented by the scattering light intensity, the scattering light intensity was integrated over a circle  $(0, r)$  for  $r=1.64 \mu\text{m}$  and over a ring  $(r, r+\Delta r)$  for the rest cases, where  $\Delta r$  was set to be  $1 \mu\text{m}$ , as shown in Fig. 3(a). By doing so, the concentration of MNPs at different areas can be derived by calculating the corresponding integrated scattering light intensities. In Fig. 3(b), we showed the radial distributions of the integrated

scattering light intensity at different times after the laser beam was turned on. It can be seen that more and more MNPs were pushed out of the laser spot center and accumulated at the edge of the laser spot. At  $t=5 \text{ s}$ , the scattering light intensity at the laser spot center dropped to nearly zero, indicating MNPs in this area were depleted completely. No recovery of the scattering light intensity was observed when the laser light was turned on, implying that the Soret feedback effect was suppressed.

Apart from the thermal diffusion and mass diffusion, the optical forces exerted on MNPs dominate the dynamics of MNPs near the center of the laser spot. For Rayleigh scattering, the optical forces are determined by the polarizability of the particle at the laser wavelength and the spatial distribution of the optical field. The optical forces can be classified into the dissipative force (scattering and absorption forces),  $F_D = (1/2)k\alpha''(\omega)|E_0|^2$ , which always pushes nanoparticles out of the focal region, and gradient force  $F_G = (1/4)\alpha'(\omega)\nabla|E_0|^2$  [21,22]. At 532 nm, the imaginary part of the permittivity of MNPs is much larger than its real part. As a result, the dissipative force is much larger than the gradient force and it dominates the dynamics of MNPs [23]. As can be seen in Fig. 2, most of MNPs in the laser spot center were pushed out by the dissipative force and a depletion area was formed in the laser spot center. Occasionally, some MNPs drifting back to the laser

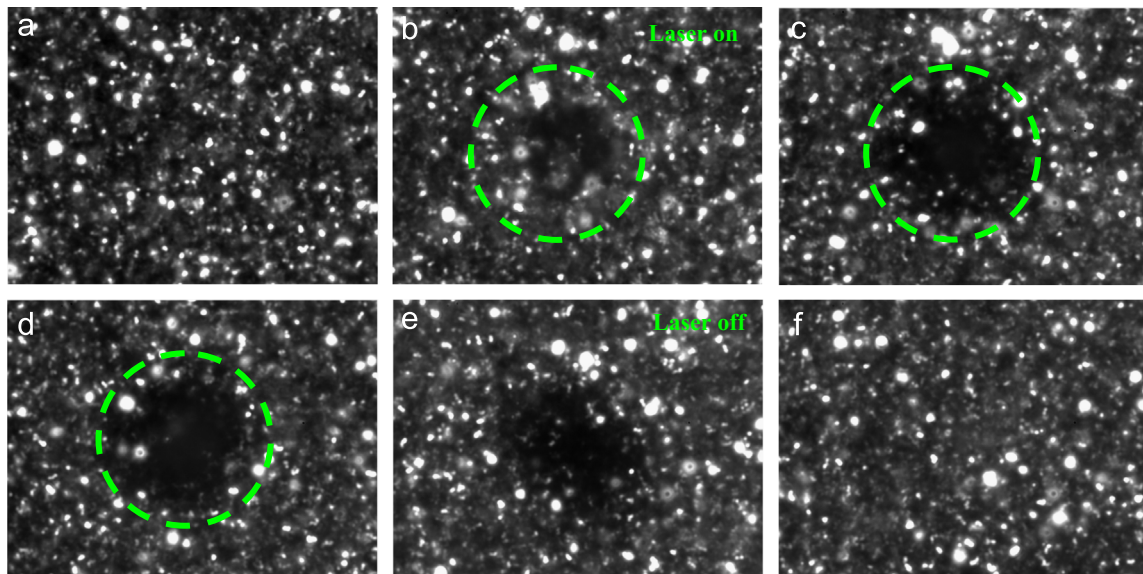


**Fig. 2.** Dynamics of MNPs under the irradiation of focused laser beam. (a) The initial distribution of MNPs. ((b)–(d)) The distribution of MNPs at 0.05, 0.4, and 5 s after a focused laser beam was turned on. ((e) and (f)) The distribution of MNPs at 0.05, 1 s after the laser light was turned off. (For interpretation of the references to color in this figure legend, the reader is referred to the web version of this article.)

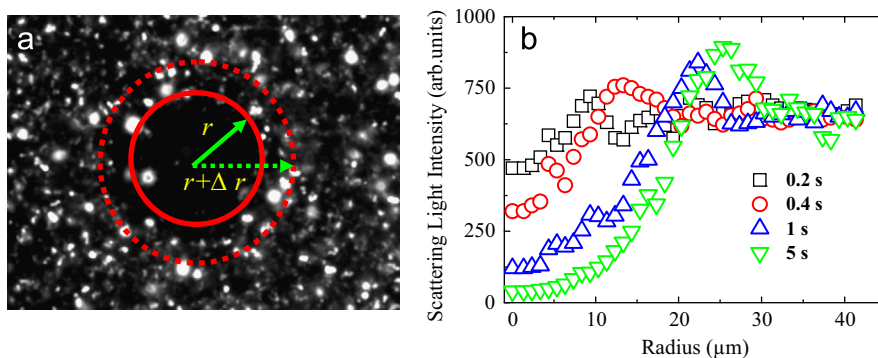


**Fig. 3.** (a) Schematic showing the integration of the scattering light intensity over a circle  $(0, r)$  for  $r=1.64 \mu\text{m}$  and over a ring  $(r, r+\Delta r)$  for the rest cases. (b) Evolution of the integrated scattering light intensity distribution along the radial direction after the laser light was turned on. Here,  $\Delta r$  was chosen to be  $1 \mu\text{m}$ . (For interpretation of the references to color in this figure legend, the reader is referred to the web version of this article.)

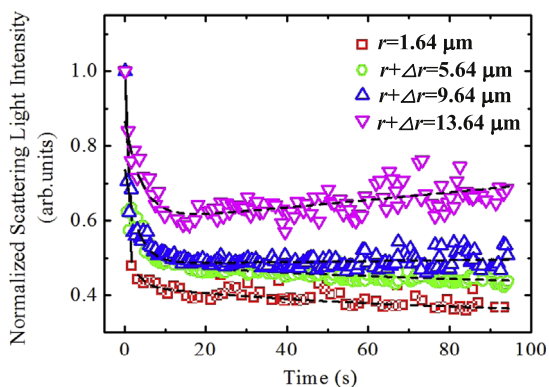


**Fig. 4.** Evolution of the integrated scattering light intensity over a circle ( $0, r$ ) for  $r=1.64 \mu\text{m}$  and over a ring ( $r, r+\Delta r$ ) for the rest cases after the laser light was turned on. Here,  $\Delta r$  was chosen to be  $4 \mu\text{m}$ . The black lines indicate the fitting of the experimental data. (For interpretation of the references to color in this figure legend, the reader is referred to the web version of this article.)

spot center were quickly pushed away by the strong dissipative force.

Fig. 4 shows the evolution of scattering light intensities with increasing laser irradiation time in four areas with  $r+\Delta r=1.64, 5.64, 9.64$  and  $13.64 \mu\text{m}$ , respectively. In each case, the maximum scattering light intensity has been normalized to one. For  $r+\Delta r < 9.64 \mu\text{m}$ , the scattering light intensity decreased sharply when the laser was switched on, indicating that MNPs were rapidly pushed out of these areas. For  $r+\Delta r=9.64 \mu\text{m}$ , the scattering light intensity decreased only to 0.5. It implied that the dissipative force was weak at the edge of the laser spot. However, for  $r+\Delta r=13.64 \mu\text{m}$ , the scattering light intensity decreased to 0.65 at 10 s and then gradually increased to 0.7. In this process, a small quantity of MNPs pushed out of the laser spot center by the optical forces would return to this region. However, taking the direction of the optical forces and the thickness of the sample cell ( $50 \mu\text{m}$ ) into account, the influence of this behavior on the concentration of MNPs on the focal plane was negligible. Comparing with the cases of  $r < 9.64 \mu\text{m}$ , the ring with  $r+\Delta r=13.64 \mu\text{m}$  was located in the outer edge of the laser spot where the dissipative force can be neglected. The dynamics of MNPs in this area was mainly governed by thermal diffusion and mass diffusion. Since the mass diffusion of the MNPs is caused by the thermal diffusion of MNPs, the whole dynamics can be divided into two processes which are dominated by thermal diffusion and mass diffusion, respectively.

By fitting the curve for  $r+\Delta r=13.64 \mu\text{m}$  with a combination of an exponential decay function and an exponential growth function, we extracted the time constants  $t_1 \sim 0.091 \text{ s}$  and  $t_2 \sim 408 \text{ s}$ . Taking the experimental conditions into account, we have  $\alpha \sim 25.9 \text{ cm}^{-1}$ ,  $\chi \sim 10^{-3} \text{ cm}^2/\text{s}$ ,  $\rho C_p \sim 1 \text{ J}/\text{cm}^3 \text{ K}$  and  $I \sim 662 \text{ W}/\text{cm}^2$ . By substituting all these parameters into Eq. (7), we obtained  $D_T \sim 6.4 \times 10^{-7} \text{ cm}^2/\text{K s}$ . Since the size of  $R$  was  $1.2 \text{ cm}$ , we got  $\kappa \sim 6.86/\text{cm}^2$ . Based on Eq. (12), the mass diffusion coefficient can be derived to be  $D \sim 3.58 \times 10^{-4} \text{ cm}^2/\text{s}$ . Using the values for the thermal and mass diffusion coefficients derived above, we can easily obtain the value of the Soret coefficient, which is defined as  $S_T = D_T/D$ , to be  $1.79 \times 10^{-3} \text{ K}^{-1}$ . This value is in good agreement with those measured by other techniques [24,25].

## 5. Conclusions

The dynamics of  $\text{Fe}_3\text{O}_4$  MNPs under the irradiation of tightly focused laser beam was investigated and the Soret coefficient for MNPs in magnetic colloid was extracted by using the dark-field

microscopy. The experimental results revealed that the dynamics of MNPs under the irradiation of focused laser beam was dominated by optical forces near the center of the laser spot and governed by thermal and mass diffusion at about  $10 \mu\text{m}$  from the laser spot center. The obtained experimental results interpreted our previous observation of the assembly of three-dimensional crystal by utilizing the giant nonequilibrium depletion force induced by a single tightly focused laser beam and provided a convenient technique to measure the Soret coefficient of nanoparticles suspended in colloids.

## Acknowledgements

The authors are grateful to Professor Sheng Lan for valuable discussions. The research was financially supported by the Natural Science Foundation of Guangdong province (Grant No. S20120-40007719).

## References

- [1] S.H. Chung, A. Hoffmann, S.D. Bader, C. Liu, B. Kay, L. Makowski, L. Chen, Biological sensors based on Brownian relaxation of magnetic nanoparticles, *Appl. Phys. Lett.* 85 (2004) 2791.
- [2] G.V. Kurlyandskaya, M.L. Sanchez, B. Hernandez, V.M. Prida, P. Gorria, M. Tejedor, Giant-magnetoimpedance-based sensitive elements as a model for biosensors, *Appl. Phys. Lett.* 82 (2003) 3053–3055.
- [3] M. Strömberg, K. Gunnarsson, S. Valizadeh, P. Svedlindh, M. Strømme, Aging phenomena in ferrofluids suitable for magnetic biosensor applications, *J. Appl. Phys.* 101 (2007) 023911.
- [4] S. Pu, X. Chen, L. Chen, W. Liao, Y. Chen, Y. Xia, Measurement of the refractive index of a magnetic fluid by the retroreflection on the fiber-optic end face, *Appl. Phys. Lett.* 87 (2005) 021901.
- [5] H.E. Horng, C.Y. Hong, S.L. Lee, C.H. Ho, S.Y. Yang, H.C. Yang, Magneto-chromatics resulted from optical gratings of magnetic fluid films subjected to perpendicular magnetic fields, *J. Appl. Phys.* 88 (2000) 5904.
- [6] C.Y. Hong, H.E. Horng, I.J. Jang, J.M. Wu, S.L. Lee, W.B. Yeung, H.C. Yang, Magneto-chromatic effects of tunable magnetic fluid grating, *J. Appl. Phys.* 83 (1998) 6771.
- [7] W. Liao, X. Chen, Y. Chen, S. Pu, Y. Xia, Q. Li, Tunable optical fiber filters with magnetic fluids, *Appl. Phys. Lett.* 87 (2005) 151122.
- [8] T. Liu, X. Chen, Z. Di, J. Zhang, X. Li, J. Chen, Tunable magneto-optical wavelength filter of long-period fiber grating with magnetic fluids, *Appl. Phys. Lett.* 91 (2007) 121116.
- [9] J.J. Chieh, S.Y. Yang, H.E. Horng, C.Y. Hong, H.C. Yang, Magnetic-fluid optical-fiber modulators via magnetic modulation, *Appl. Phys. Lett.* 9 (2007) 133505.
- [10] S. Pu, X. Chen, Y. Chen, Y. Xu, W. Liao, L. Chen, Y. Xia, Fiber-optic evanescent modulator using a magnetic fluid as the cladding, *J. Appl. Phys.* 99 (2006) 093516.
- [11] J.W. Seo, S.J. Park, K.O. Jang, An experimental study of light modulator using magnetic fluid, *J. Appl. Phys.* 85 (1999) 5956.
- [12] H.E. Horng, C.S. Chen, K.L. Fang, S.Y. Yang, J.J. Chieh, C.Y. Hong, H.C. Yang, Tunable optical switch using magnetic fluids, *Appl. Phys. Lett.* 85 (2004) 5592.
- [13] C.Y. Hong, Optical switch devices using the magnetic fluid thin films, *J. Magn. Mater.* 201 (1999) 178–181.
- [14] R.M. Erb, H.S. Son, B. Samanta, V.M. Rotello, B.B. Yellen, Magnetic assembly of colloidal superstructures with multipole symmetry, *Nature* 457 (2002) 999–1002.
- [15] B.B. Yellen, O. Hovorka, G. Friedman, Arranging matter by magnetic nanoparticle assemblers, *Proc. Nat. Acad. Sci. U.S.A.* 102 (2005) 8860–8864.
- [16] J. Ge, Y. Hu, M. Biasini, W.P. Beyermann, Y. Yin, Superparamagnetic magnetite colloidal nanocrystal clusters, *Angew. Chem. Int. Ed.* 46 (2007) 4342–4345.
- [17] J. Ge, Y. Yin, Magnetically tunable colloidal photonic structures in alkanol solutions, *Adv. Mater.* 20 (2008) 3485–3491.
- [18] H.D. Deng, G.C. Li, H.Y. Liu, Q.F. Dai, L.J. Wu, S. Lan, A.V. Gopal, V.A. Trofimov, T.M. Lysak, Assembling of three-dimensional crystals by optical depletion force induced by a single focused laser beam, *Opt. Express* 20 (2012) 9616–9623.
- [19] N.V. Tabiryan, W. Luo, Soret feedback in thermal diffusion of suspensions, *Phys. Rev. E: Stat. Nonlinear Soft Matter Phys.* 57 (1998) 4431–4440.
- [20] J. Lenglet, A. Bourdon, J.C. Bacri, G. Demouchy, Thermodiffusion in magnetic colloids evidenced and studied by forced Rayleigh scattering experiments, *Phys. Rev. E: Stat. Nonlinear Soft Matter Phys.* 65 (2002) 031408.
- [21] J.R. Arias-Gonzalez, M. Nieto-Vesperinas, Optical forces on small particles: attractive and repulsive nature and plasmon-resonance conditions, *J. Opt. Soc. Am. A: Opt. Image Sci. Vis.* 20 (2003) 1201–1209.
- [22] H. Xu, M. Käll, Surface-plasmon-enhanced optical forces in silver nanoaggregates, *Phys. Rev. Lett.* 89 (2002) 246802.

- [23] Z.M. Meng, H.Y. Liu, W.R. Zhao, W. Zhang, H.D. Deng, Q.F. Dai, L.J. Wu, L. Sheng, A.V. Gopal, Effect of optical forces on the transmission of magnetic fluids investigated by Z-scan technique, *J. Appl. Phys.* 106 (2009) 044905.
- [24] S.I. Alves, A. Bourdon, A.M. Figueiredo Neto, Investigation of the Soret coefficient in magnetic fluids using the Z-scan technique, *J. Magn. Magn. Mater.* 289 (2005) 285–288.
- [25] S. Alves, F.L.S. Cuppo, A. Bourdon, A.M. Figueiredo Neto, Thermodiffusion of magnetite nanoparticles in ferrofluid-doped micellar systems and in ferrofluids investigated by using the single-beam Z-scan technique, *J. Opt. Soc. Am. B: Opt. Phys.* 23 (2006) 2328–2335.